Liquid Crystals

Publication details, including instructions for authors and subscription information:
http://www.informaworld.com/smpp/title~content=t713926090

The antiferroelectric TGB phase: textures, field-induced effects and microscopic model

J. G. Meier; P. Rudquist; A. S. Petrenko; J. W. Goodby; S. T. Lagerwall

To cite this Article Meier, J. G. , Rudquist, P. , Petrenko, A. S. , Goodby, J. W. and Lagerwall, S. T.(2002) 'The antiferroelectric TGB phase: textures, field-induced effects and microscopic model', Liquid Crystals, 29: 2, 179 — 189

To link to this Article: DOI: 10.1080/02678290110095613

URL: http://dx.doi.org/10.1080/02678290110095613

Liquid Crystals, 2002, Vol. 29, No. 2, 179–189

Taylor & Francis
Taylor & Francis Group

The antiferroelectric TGB phase: textures, field-induced effects and microscopic model

J. G. MEIER*, P. RUDQUIST, A. S. PETRENKO†, J. W. GOODBY†
and S. T. LAGERWALL

Department of Microelectronics and Nanoscience,
Chalmers University of Technology, SE-41296 Göteborg, Sweden
†Department of Chemistry, University of Hull, Hull HU6 7RX, UK

(*Received 18 May 2001; in final form 20 August 2001; accepted 30 August 2001*)

By studying the optical textures and the field-induced effects of the recently discovered $TGBC_A$ phase we have developed a qualitative model of the microscopic organization of the phase. Inside the smectic blocks, the molecular tilt plane of the local anticlinic structure is perpendicular to the helix of the $TGBC_A$ phase. The grain boundaries consist of a regular lattice of $+1/2$ and $-1/2$ dispirations; i.e. unit screw dislocations combined with half unit disclinations. Whereas all screw dislocations have the same sign, the sign of the half unit disclinations alternates in adjacent dispirations. Hence, in the grain boundaries the molecular tilt plane between adjacent dispirations is alternately parallel and perpendicular to the TGB helix.

1. Introduction

In 1972 de Gennes [1] described the nematic–smectic A transition in liquid crystals by analogy to the conductor–superconductor transition in metals. According to this analogy, the introduction of chirality to the layered SmA phase is analogous to the application of a magnetic field to a superconductor. If the nematic phase is chiral, its twist is then expelled at the N*–SmA* transition, just as the magnetic field is expelled by the superconductor. However, at sufficiently strong twisting power, a new structure may appear in which the layered phase is penetrated by a regular pattern of twist line singularities, just as the superconductor may be penetrated by a pattern of singular flux lines. In 1988 Renn and Lubensky [2] developed a specific model of this structure which they called the twist grain boundary (TGB) phase, describing a liquid crystal phase between the N* and SmA* phases with regularly spaced grain boundaries of screw dislocations. The screw dislocations are parallel to each other within each grain boundary, but are rotated by a fixed angle between successive grain boundaries. Since the screw dislocations form a regular lattice, the TGB phase may be seen as a liquid crystal analogue of the Abrikosov flux lattice phase found in type-II superconductors. A short time later, in 1989, Goodby *et al.* [3, 4] reported the discovery of the TGBA phase existing between the SmA* and the isotropic phases. X-ray studies performed by Srajer *et al.* [5] confirmed that the essential features and the physical properties of the TGBA phase were very well described by the Renn-Lubensky model.

Further studies led to the prediction of two more TGB phases in the vicinity of the N*–SmA*–SmC* triple point, viz. the TGBC (expulsion of the smectic C* helix in the blocks) and $TGB\tilde{C}$ phases (incorporation of the smectic C* helix in the blocks) [6], and the subsequent discovery of the TGBC phase by Nguyen *et al.* [7]. For the TGBC phase a number of special cases has been proposed and/or discovered; these are distinguished by (a) the commensurability or incommensurability of the number of sheets of screw dislocations with respect to the pitch length of the phase [8], (b) the inversion of the handedness of the helix in the TGBC phase on changing the temperature [9], and (c) the formation of a 2D modulated structure [10].

Whereas the Abrikosov phase in superconductors consists of a two-dimensional lattice of vortex lines, the analogous liquid crystal phases are geometrically much more complicated, as the singular lines can only be parallel along one direction; but sets of such directions twist to create a three-dimensional periodic structure containing blocks or slabs of a two-dimensional liquid. Also the distinction between different ‘Abrikosov’ phases

---

*Author for correspondence; e-mail: jgm@fy.chalmers.se

Liquid Crystals ISSN 0267-8292 print/ISSN 1366-5855 online © 2002 Taylor & Francis Ltd
http://www.tandf.co.uk/journals
DOI: 10.1080/02678290110095613

is unique for liquid crystals, i.e. the orthogonal/tilted and helical/non-helical organization of the molecules within each slab.

TGB phases mediate transitions from the isotropic or chiral nematic state to the smectic state. Generally the structures of TGB phases have been found to be based on the structures of the smectic phases that they either replace or to which they transform upon cooling. It also appears that TGB phases often occur in conjunction with blue phases (their nematic counter parts), the SmC^*_α, the $\mathrm{SmC}^*_{1/4}$ and the $\mathrm{SmC}^*_{1/3}$ subphases (the latter two with a unit cell corresponding to four and three layers, respectively) and the antiferroelectric $\mathrm{SmC}^*_\mathrm{A}$ phase [11].

Recently a twist grain boundary phase with a local antiferroelectric structure ($\mathrm{TGBC_A}$) has been discovered in the compound depicted in figure 1 [12, 13]. In the present paper we discuss the textures and the electric field-induced effects of this same compound. Based on the observations we have developed a qualitative model for the molecular arrangement in the $\mathrm{TGBC_A}$ phase.

2. Experimental

The liquid crystal was studied in glass cells of 1, 2, 4 and 22 µm thickness. The 2 and 4 µm cells were manufactured by E.H.C. (Japan), and the cells with 1 and 22 µm gaps were self-made. All the cells have transparent ITO electrodes and polyimide alignment layers buffed antiparallel to impose planar anchoring conditions. The textures were observed and recorded using a Photomicroscope III (Zeiss) in conjunction with a Mettler FP52 hot stage and temperature control unit Mettler FP5. The temperature was independently measured using a PT100 temperature sensor providing a reproducibility and stability accuracy of 0.01 K for the hot stage subset. The electro-optic response was detected by means of a photodiode attached to the photo tube of the microscope. The electric field for the electro-optic experiments was generated using a leader functiongenerator LFG 1300 and voltage amplifier F20ADI from FLC Electronics. The current, the optical response and the applied voltage were simultaneously recorded by means of a four channel digital memory oscilloscope (Tektronix TDS 540). The selective reflection wavelengths were measured using a Shimadzu UV-3100 UV/VIS/NIR spectrophotometer fitted with a Mettler FP52 hot stage and controller unit.

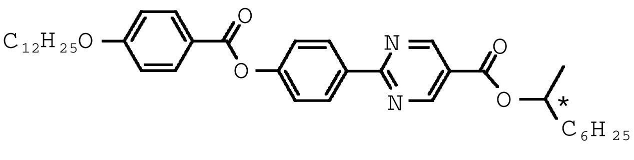

Figure 1. Molecular structure of the compound studied. The phases and transition temperatures are: isotropic 93.1 SmQ 92.9 $\mathrm{TGBC_A}$ 91.6 $\mathrm{SmC}^*_\mathrm{A}$ 68.3 Cr (°C); m.p. 86.4°C.

3. Results

3.1. *Textures*

Upon cooling from the isotropic liquid predominantly a Grandjean-like texture developed in all cells, see figure 2(*c*). Characteristic of this Grandjean-like texture is that no extinction of light is achieved for any settings of the crossed polarizers; it shows strong optical rotation and selective reflection in the visible and, thus, reminds one of the Grandjean texture of a cholesteric liquid crystal. In this texture the helix has a submicron pitch and the helix axis of the $\mathrm{TGBC_A}$ phase is perpendicular to the cell surfaces (analogous to the cholesteric Grandjean texture). Hence the optic axis, being coaxial with the TGB helix, is along the direction of observation in the Grandjean texture. In the 2, 4 and 22 µm thick cells, some areas of the sample also exhibited a type of focal-conic texture where light extinction could be observed between crossed polarizers. However, such focal-conic domains did not appear on heating from the $\mathrm{SmC}^*_\mathrm{A}$ phase. These domains remind one of focal-conics with an optic axis more or less parallel to the cell surfaces. Both types of textures were persistent throughout the whole temperature range of the $\mathrm{TGBC_A}$ phase. However, in a cell of approximately 1 µm thickness, only the Grandjean texture of the TGB phase appeared upon cooling from the isotropic state, and not the focal-conic texture. Thus the Grandjean texture is actually surface-stabilized in very thin cells. A continuous decrease of temperature causes discrete changes of colour in the Grandjean domains as the pitch increases. This is a result of the fixed confining boundary conditions. A discussion of the corresponding textures for the TGBA and TGBC phase can be found in [14] and references therein.

At the TGB–$\mathrm{SmC}^*_\mathrm{A}$ transition, the $\mathrm{SmC}^*_\mathrm{A}$ phase forms a fan-shaped texture which may be likened to a random bookshelf structure. On heating again into the TGB phase, the front of the phase transition moves preferably along the radii of the fans of the antiferroelectric smectic C^*_A phase, figure 2(*a*). Very pronounced also is the pre-transitional discontinuous change in birefringence colour in the focal-conic domains, most probably due to the nucleation of the TGB phase at the bottom surface of the cell. In the transition from the $\mathrm{SmC}^*_\mathrm{A}$ to the TGB phase only the Grandjean planar texture is obtained, but no focal-conic like domains, figure 2(*b*). This can be explained by assuming that the first layers of molecules are largely locked at the surfaces which support the planar alignment. Therefore, the boundaries make the smectic layers form perpendicularly to the glass plates in the $\mathrm{SmC}^*_\mathrm{A}$ phase (bookshelf geometry). At the $\mathrm{SmC}^*_\mathrm{A}$ to $\mathrm{TGBC_A}$ transition, this surface ordering of the smectic layers is maintained and forces the breaking of the layered structure to occur in planes parallel to the cell

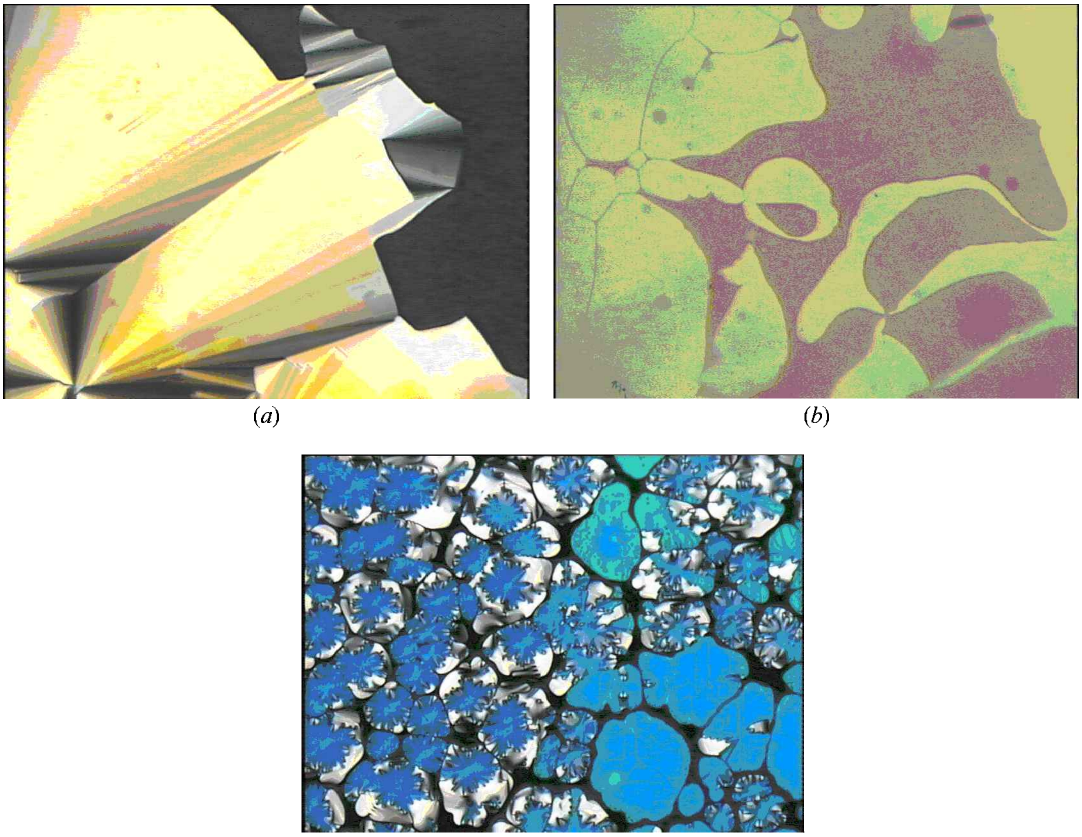

(*a*) (*b*)

(*c*)

Figure 2. The textures of the TGBC$_A$ phase depend on the history of the sample. Coming from the fan-shaped SmC$_A^*$, only the Grandjean texture of TGBC$_A$ is formed. In the beginning the Grandjean domains are very dark due to the long pitch (*a*) and become more coloured when the pitch decreases at higher temperature (*b*). However, on cooling from the isotropic phase both Grandjean and focal-conic domains appear (*c*). The alignment layers of the cell promote planar boundary conditions (director parallel to the glass plates). (*a*) Transition from the fan-shaped SmC$_A^*$ to the TGBC$_A$ phase, on heating. (*b*) TGBC$_A$ phase formed upon heating from the SmC$_A^*$ phase; only the Grandjean texture develops. (*c*) Transition from the isotropic liquid to the TGBC$_A$ phase; Grandjean planar and focal-conic-like domains develop.

surfaces. Therefore, the nucleation of the TGB phase from a bookshelf SmC$_A^*$ structure results 'automatically' in the Grandjean texture on heating from the C$_A^*$.

The pitch of the TGB helix was determined by measuring the wavelength of the selectively reflected light observed as a dip in the transmission spectrum at normal incidence in the Grandjean texture (figure 3). In this geometry the spectrometer reading λ is related to the helical pitch p of the liquid crystal phase according to $\lambda = \bar{n}p$. Assuming an average refractive index $\bar{n}$ of 1.5, the pitch of the helical superstructure varies from about 500 to 330 nm within a temperature range of 1.7 K.

In addition to what has been reported earlier [12, 13], we observed the formation of yet another texture in the close vicinity of the clearing temperature. Upon very slow cooling (*c*. 0.05 K min^{-1}) from the isotropic liquid, or heating (*c*. 0.1 K min^{-1}) from the TGB phase, a mosaic-like texture with low birefringence develops

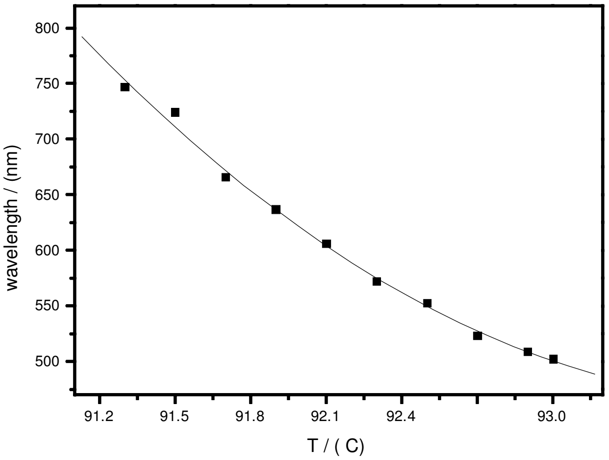

Figure 3. Wavelengths of the selectively reflected light from the Grandjean planar texture of the TGBC$_A$ phase depending on temperature.

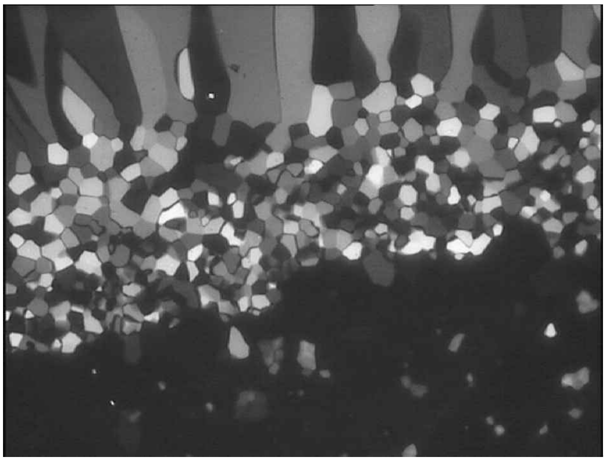

Figure 4. Texture of the SmQ phase.

(figure 4). This blue phase-like texture (though not as colourful) is very sensitive to any disturbance and its temperature interval is about 0.2 K. The texture may tentatively be attributed to the so-called SmQ phase [15], which has been reported to exist between the SmC$_A^*$ and the isotropic phase in certain materials. Levelut *et al.* [16] performed extensive X-ray studies on the SmQ phase and identified four different structure types all belonging to the class of defect crystals. Two of those structures could be described as *arrays of twist grain boundaries in an antiferroelectric smectic* [16].

3.2. *Electro-optic experiments*

In order to get more information about the detailed molecular arrangement of the TGBC$_A$ phase we studied the response of the material to electric fields. Characteristic textures of the SmC$_A^*$ and the TGBC$_A$ phase under an applied electric field and the related electro-optic responses can be distinguished, as shown in figure 5. The photomicrographs depict a part of the cell inside and outside the electrode area. The graphs show the applied field (dashed line) and the resulting current (solid line) and optical (dotted line) response. The scale of the optical response in figure 5 (*b*) has been enlarged by a factor of 10 for better perceptibility. The optical responses in figures 5 (*a*) and 5 (*c*) are of about the same amplitude and given with the same scale. The data presented in figure 5 (*a*) were taken in the SmC$_A^*$ phase and show typical electro-optic characteristics of an antiferroelectric liquid crystal—double peak of the current response per half period of the driving field and three-state optical switching. The corresponding photograph, figure 5 (*d*), shows the field-free focal-conic texture (unaddressed area to the right) and the field-induced ferroelectric state (left) of the antiferroelectric liquid crystal. Note that in the addressed area the liquid crystal is aligned with its smectic layer normal more or less along the rubbing direction of the alignment layers (parallel to the edge of the electrode), whereas in the unaddressed area the smectic layer normal varies and is not correlated to the

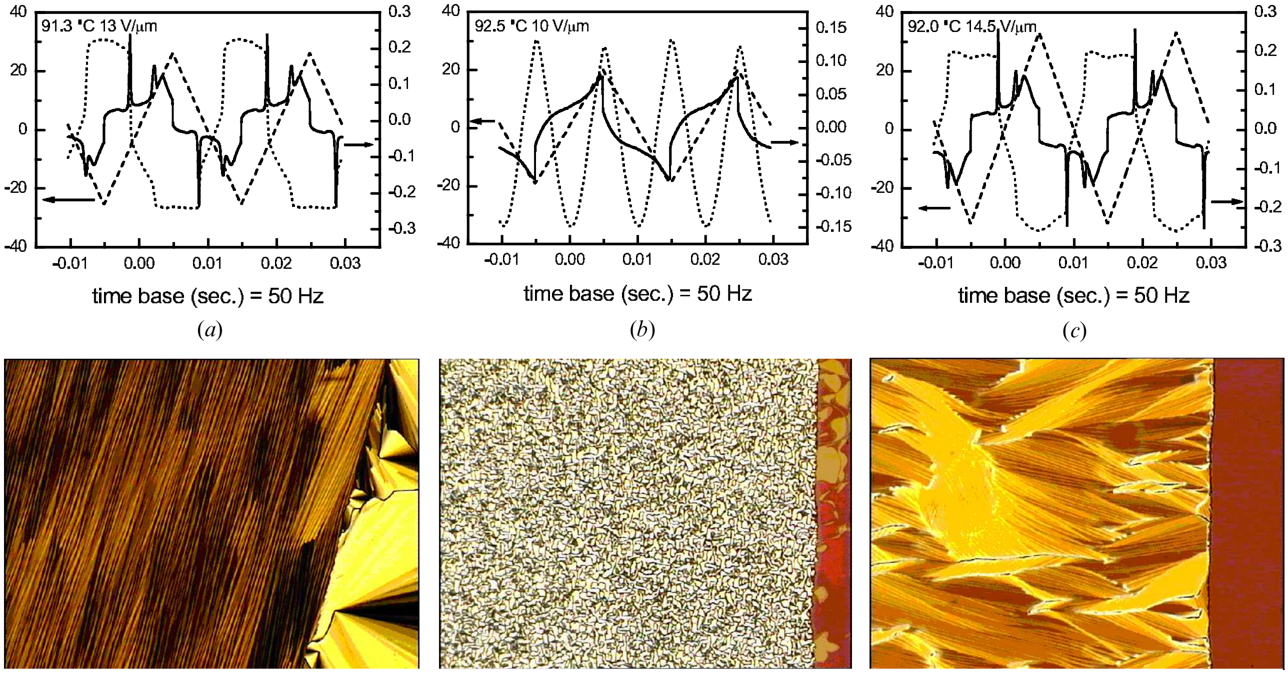

(*a*) (*b*) (*c*)

(*d*) (*e*) (*f*)

Figure 5. The electric field-induced textures and their electro-optic signatures. The liquid crystal is in the SmC$_A^*$ phase in (*a*)/(*d*), in the TGB phase in (*b*)/(*e*) and (*c*)/(*f*).

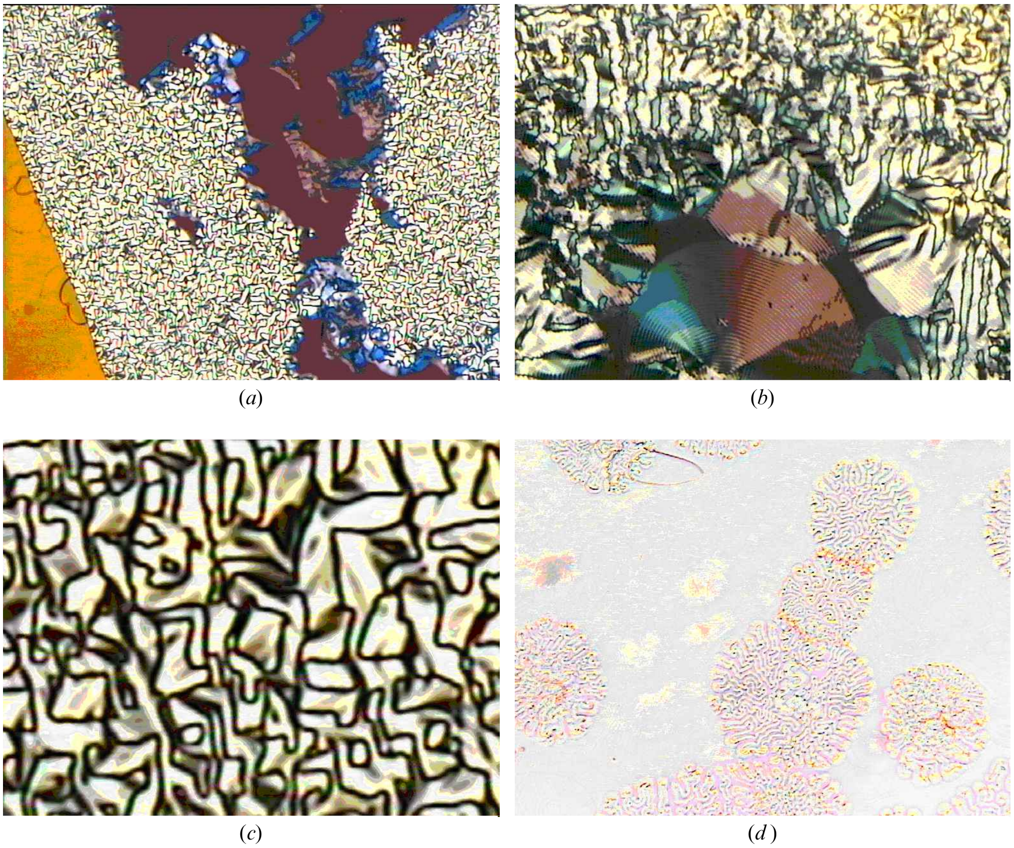

Figure 6. Electric field-induced transition form the Grandjean planar texture to the focal-conic or fingerprint texture of the TGBC$_A$ phase. (*a*) 2 μm cell, crossed polarizers, *c.* 60×; the blueish domains contain a stripe pattern and the white areas are focal-conic-like. (*b*) 2 μm cell, crossed polarizers, *c.* 100×; focus on such a blueish area—the fan-shaped domain nucleates within a Grandjean area. The pitch bands suggest a helix parallel to glass plates. (*c*) 2 μm cell, crossed polarizers, *c.* 250×; focus on the white areas—a focal-conic texture is apparent. (*d*) 22 μm cell, no polarizers, *c.* 60×; field-induced transition from the Grandjean to a typical fingerprint texture, suggesting a change of the helix axis from perpendicular to parallel to the cell surfaces.

rubbing. Figures 5 (*b*) and 5 (*e*) show the same arrangement for the TGBC$_A$ phase. Outside the electrode area (right), the phase exhibits a Grandjean planar texture; i.e. the smectic slabs form a helix which is perpendicular to the cell surfaces. Inside the electrode area (left) a field-induced focal-conic-like texture (to be discussed later, cf. figure 6) is apparent. Hence, the weak optical response of this random texture is caused by a small change in birefringence fluctuating with twice the frequency of the driving field. This is characteristic for a dielectric response; for instance, the deformation/unwinding of a helix according to the field. On increasing the a.c. field strength the TGB helix completely unwinds. An electro-optic response develops, figure 5 (*c*), which is identical to the signature of a typical antiferroelectric liquid crystal—compare figures 5 (*a*) and 5 (*c*). Note that if the TGB phase has either a SmA or SmC order in its smectic slabs, an electroclinic or a ferroelectric response should be obtained†. Therefore we may conclude that *the found TGB phase has a local antiferroelectric and anticlinic structure* (SmC$^*_A$ order).

In more detail, the electro-optic response in the TGB phase may be described as follows. On applying an electric field exceeding a certain threshold parallel to the helix-axis of the TGB Grandjean texture, the texture changes into a focal-conic-like texture in thin cells or a fingerprint texture (focal-conics were seen as well) in thick cells (figure 6). The field-induced transformation from Grandjean to focal-conic is preceded by an increase of the helical pitch, indicated by the change in colour of

---

† For frequencies below *c.* 0.5 Hz the TGB structure reappears when the applied field passes through zero indicating the dynamic aspects of that field-induced effect, i.e. the TGB structure unwinds and rewinds with twice the frequency of the low frequency applied a.c. field, rather than switching from one ferroelectric state to the other.

the Grandjean texture. The pitch changes in discrete steps observed as growing domains with different colour, in a very similar manner to the way it changes with temperature. This is illustrated in the micrographs shown in figure 6. The lower left corner of figure 6 (*a*) shows the Grandjean texture outside the electrode area which is not subjected to the electric field. In the electrode area there are field-induced focal-conic domains (bright), as well as purple areas of Grandjean domains which have not yet transformed into the focal-conic texture. The difference in colour with respect to the field-free areas is due to a longer pitch of the helix in the presence of the electric field. The field-induced transformation from Grandjean to fan-shaped focal-conic texture is connected with the appearance of regular pitch bands parallel to the growing direction of the fan. These pitch bands suggest the presence of a helix with a pitch of several microns now lying parallel to the cell surfaces. This is also supported by the observation of a very typical field-induced fingerprint texture in thick cells, figure 6 (*d*). On further development of the domains the pitch bands become less and less visible.

In conclusion, the Grandjean planar texture does not exhibit any measurable internal electro-optic response other than the field-induced step-wise change of colour. Furthermore, the transformation into the focal-conic domains depends only on the amplitude of the electric field and works with an a.c. as well as with a d.c. field. The field-induced focal-conic texture exhibits a dielectric optical response under an applied a.c. field. We suggest that the field-induced transition from Grandjean to focal-conic texture is due to a 90° reorientation of the helix axis of the structure, from being perpendicular to essentially parallel to the glass plates. This would also be similar to the Grandjean to fingerprint or focal-conic transition in cholesteric liquid crystals. Furthermore, just as in the cholesteric case, the field-induced focal-conic texture is metastable and relaxes very slowly back (within hours) to the Grandjean texture when the field is removed.

In figure 7 a phase diagram is shown. This was obtained from electro-optic experiments and texture observations, introducing the electric field as the state variable in order to shed more light on each of the field-induced transformations and their relation to one another. Since the introduced state variable **E** is of vectorial nature, it should be noted that the resulting diagram is strongly dependent on the direction of **E** with respect to the liquid

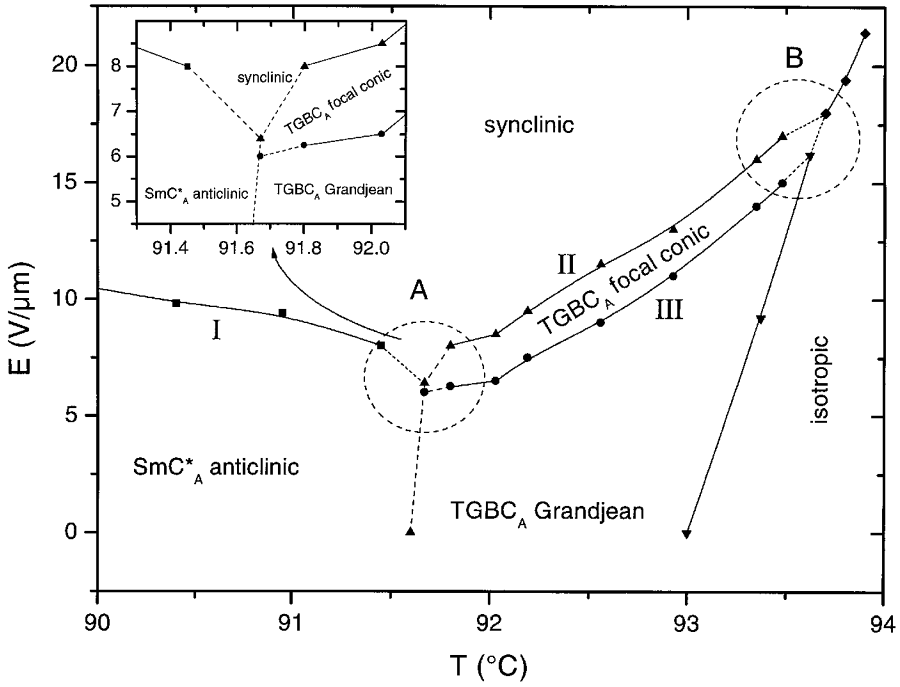

Figure 7. The field induced states.

crystal geometry. The diagram shows the thresholds for the field-induced transformation of the Grandjean to the focal-conic texture of the $TGBC_A$ phase, the subsequent TGB helix unwinding and the anticlinic to synclinic transition of the SmC_A^* phase depending on temperature and applied electric field strength. At sufficiently high field strengths the ferroelectric states of the antiferroelectric structure are stabilized. Because **E** is a state variable and influences the total energy of the system, the $TGBC_A$ focal-conic texture can be considered as related to an independent phase in the given coordinate system and geometry. The slope of curve I, marking the synclinic to anticlinic transition of the SmC_A^* phase, is of opposite sign and with different steepness to that of curve II, marking the transition from the $TGBC_A$ focal-conic state to the synclinic state. If the $TGBC_A$ focal-conic state were identical with the anticlinic state of the antiferroelectric phase, i.e. if the TGB helix were unwound, one would expect to find line II continued with basically the same slope for $T < 91.6$°C as in line I. Furthermore, in each of the areas marked with A and B we can identify two triple points. In A the triple points are formed by (i) SmC_A^* anticlinic, $TGBC_A$ Grandjean, $TGBC_A$ focal-conic and (ii) SmC_A^* anticlinic, $TGBC_A$ focal-conic, synclinic. In B we find the two triple points (i) $TGBC_A$ Grandjean, $TGBC_A$ focal-conic, isotropic and (ii) $TGBC_A$ focal-conic, synclinic, isotropic. Thus, at moderate fields, such as $8\,\mathrm{V\,\mu m^{-1}}$, we would, on lowering the temperature, see a transition sequence isotropic–$TGBC_A$ Grandjean–$TGBC_A$ focal-conic, and finally a transition to the field-induced synclinic state of the SmC_A^*.

On slowly cooling the sample at the transition from the developed focal-conic texture of the TGB to the anticlinic state of the SmC_A^* phase (area marked with A) while maintaining the electric field strength, there is a significant change of texture when the SmC_A^* phase appears, cf. figure 8. The new texture is the same as that of the SmC_A^* anticlinic state. This change observed at the transition is further evidence that the $TGBC_A$ focal-conic state is not equivalent to the anticlinic state of the SmC_A^* phase. Curve III in figure 7, indicating the threshold for the transformation from Grandjean to focal-conic texture, has approximately the same slope as curve II which describes the electric field threshold for the transition to the synclinic state. On cooling from the isotropic phase, either the planar Grandjean, the focal-conic or the synclinic ferroelectric texture, each with its characteristic electro-optic signature, can be achieved depending on the amplitude of the applied electric field.

The phase transition from liquid crystalline state to isotropic is shifted to higher temperatures in the presence of an electric field. On applying a field, the nucleation of the SmQ phase is inhibited. This phase would appear at the lowest point ($\mathbf{E} = 0$) of the isotropic–$TGBC_A$ Grandjean line transition in figure 7 if we were dealing with equilibrium states. However, since the SmQ phase is very sensitive to any disturbance, the isotropic liquid is easily supercooled to this point. Apparently, small to moderate electric fields induce the nucleation of the Grandjean texture of the $TGBC_A$ phase at the expense of the SmQ phase. At high fields, about $20\,\mathrm{V\,\mu m^{-1}}$, the field strongly stabilizes the macroscopically polar synclinic state by almost one degree.

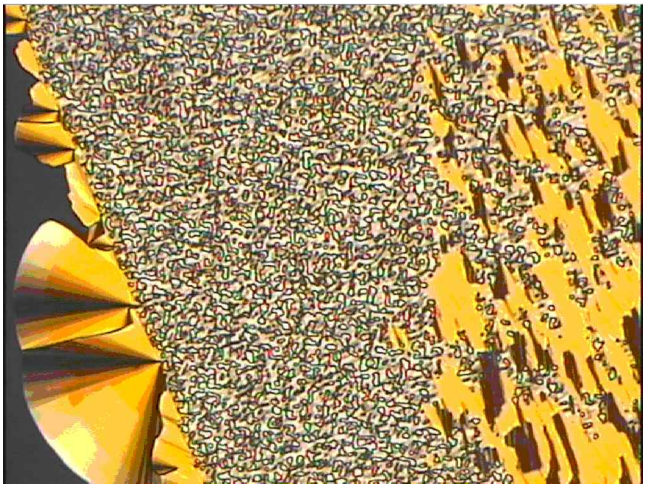
Figure 8. Transition from the $TGBC_A$ focal-conic to the SmC_A^* anticlinic state under constant electric field strength upon cooling at a very slow rate.

4. Discussion

The optical textures, the electric field effects, and the electro-optic response, as discussed in § 3, give evidence that the $TGBC_A$ phase indeed has local anticlinic, antiferroelectric order. As already known, the helical structure of a TGB phase may be characterized by: (i) the pitch along the quasi-helix axis (p); (ii) the thickness of the smectic blocks (l_b); (iii) the distance of the screw dislocations within a grain boundary (l_d) and (iv) the inclination angle between adjacent slabs ($\Delta\theta$). This also holds for the $TGBC_A$ phase, as indicated in figure 9. But let us now discuss the possible molecular organization *within* the slabs and in the *vicinity* of the grain boundaries of the $TGBC_A$ phase. The discussion below is made in terms of the orientation of the tilt plane, i.e. the plane spanned by the local director and the smectic layer normal. We come to the conclusion that the tilt plane of the local anticlinic order in the smectic slabs is always perpendicular to the helix axis of the $TGBC_A$ phase, whereas in the grain boundaries, between adjacent dispirations, the tilt plane is alternately parallel and perpendicular with respect to the helix axis.

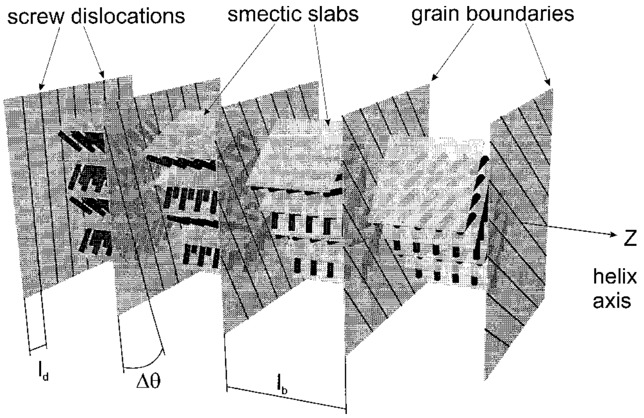

Figure 9. Schematic representation of the $TGBC_A$ model.

It is known that for electric fields applied along the smectic layers of an antiferroelectric liquid crystal, below the field-induced antiferroelectric to ferroelectric transition, the molecular tilt plane reorients into the field direction. Fukuda *et al.* [17] made conoscopic experiments on thick (≈ 100–$200\,\mu m$) freely suspended films. In such films the smectic layers are parallel to the film and the helix of the SmC_A^* is perpendicular to the film. On applying an electric field in the film plane, the helix was unwound by the field. The unwound anticlinic structure is macroscopically biaxial with the two optic axes in a plane perpendicular to the tilt plane, and the conoscopic picture directly gives the orientation of the tilt plane in relation to the direction of the applied field. As the two optic axes were found to be perpendicular to the applied field, Fukuda and co-workers could conclude that the tilt plane of the unwound structure was along the field.

Shiyong *et al.* [18] studied bookshelf aligned cells with a surface-stabilized AFLC. In such cells the SmC_A^* helix is suppressed by surface action and the tilt plane is everywhere parallel to the glass plates. On applying an electric field perpendicular to the glass plates they could at a certain threshold voltage observe a Fréedericks-like transition, earlier predicted by Qian and Taylor [19], in which the tilt plane reoriented to become essentially parallel to the field. Both the field-induced unwinding of the helix in the films and the Fréedericks transition in the bookshelf cells could at first be considered to be due to dielectric coupling ($\sim\Delta\varepsilon$), but they are in fact due to the much stronger coupling between the electric field and uncompensated electric polarization arising from antiphase fluctuations in adjacent layers [18]. As a result of this, the lowest energy state is achieved when the tilt plane is along the field at the same time as the smectic layer normal is perpendicular to the field. For simplicity we will refer to this lowest energy state by using the expression 'the tilt plane is along the electric field'. In this geometry the torque on the local $\mathbf{P}_s$ of each smectic layer, $\mathbf{P}_s \times \mathbf{E}$, is maximized which in turn amplifies any antiphase distortion and hence increases the induced net polarization. As a comparison, when the tilt plane is perpendicular to the applied field, $\mathbf{P}_s \times \mathbf{E} = 0$, and the field has essentially no influence on the structure below the Fréedericks transition and/or below the antiferroelectric to ferroelectric transition. The symmetries and tilt plane orientations of $TGBC_A$ and AFLCs in general will be treated elsewhere [20].

Let us now return to the $TGBC_A$ phase and assume that we have the same kind of coupling between the electric field and the tilt plane as in the SmC_A^* cases just described. We know that in the field-induced transformation from Grandjean to fingerprint/focal-conic textures there is a reorientation of the TGB helix from perpendicular to parallel to the glass plates. This transition can now be explained by assuming that *the tilt plane is perpendicular to the helix axis*, cf. figure 9, and hence perpendicular to the applied field in the Grandjean texture. On increasing the electric field strength we increase the electrostatic energy of the system and above a certain threshold a structure for which the tilt plane is perpendicular to the field, that is the Grandjean structure, becomes unstable. This gives the transformation from Grandjean to the focal-conic texture with a TGB helix parallel to the glass plates. In this configuration the lowest energy condition, i.e. smectic layer normal is perpendicular to the field while the tilt plane is along the field, is more or less fulfilled in about 50% (due to the helical structure) of the sample. This field-induced transition is analogous to the Grandjean to fingerprint transformation in a cholesteric liquid crystal with positive dielectric anisotropy. At a certain field strength, the Grandjean cholesteric structure with director in the plane of the cell becomes unstable, and is transformed into the fingerprint texture in which the director is alternately parallel and perpendicular to the applied field. In both the TGBC$_A$ and the cholesteric cases the helix is further unwound if the field strength is further increased. Above a certain critical field, the helix totally unwinds which results in a field-induced SmC$_A^*$ state in the TGBC$_A$ case and a homeotropic director configuration in the cholesteric case. In conclusion, the field-induced Grandjean to focal-conic/fingerprint structure of the TGBC$_A$ phase can be explained by assuming that the local tilt plane of the anticlinic structure within the smectic slabs is perpendicular to the TGB helix axis. This also means that there is no helical structure of the director along the smectic layer normal within each slab. In fact, each slab may be described as a surface-stabilized SmC$_A^*$ structure in which the two surfaces are constituted by the grain boundaries between the slabs. This picture is further supported by the absence of any electro-optic response other than the stepwise field-induced increase of the pitch, in the Grandjean configuration. If the tilt plane is perpendicular to the field, the torque on the local $\mathbf{P}_s$, and hence the electro-optic response, is minimized. If there had been a helix within the blocks, there would in addition have been a gradual change of birefringence (colour) on varying the electric field. This also suggests that the field-induced increase of the TGBC$_A$ pitch, preceding the Grandjean to focal-conic state, is connected to the action by the field on the grain boundaries.

Within the grain boundaries the situation is more complicated as a unit screw dislocation in an anticlinic smectic is automatically connected to a half-unit dispiration [17, 21]. (A pure screw dislocation would require a Burger's vector $b = 2$.)

A TGB phase can be seen as built-up of microcolumns carved in the smectic planes by the screw dislocations existing only in the vicinity of the grain boundary [22]. Figure 10 shows the *c*-director of the microcolumns of the TGBC$_A$ phase in the vicinity of a grain boundary viewed in the *x*, *y*-plane, which is the plane of the paper. Two successive smectic slabs are indicated, one above (light grey shade) and one below (darker grey shade) a grain boundary in which the screw dislocations are marked (dashed lines). Let the *c*-director be the projection of the director on the smectic layer, hence, indicating the local tilt plane. The arrows and the dotted and crossed circles indicate the direction of the *c*-director with respect to the *x*, *y*-plane being either in the plane or pointing up and down. Such a structure can only be formed by the formation of dispirations instead of pure screw dislocations (cf. figure 11). The dashed lines in figure 10 are thus dispirations. Each dispiration consists of a unit screw dislocation combined with a half-unit disclination. While all screw dislocations have the same sign, the sign of the disclinations alternates between each dispiration.

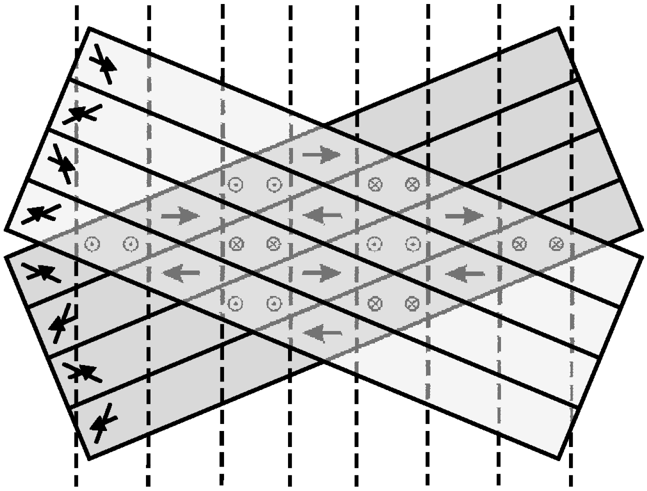

Figure 10. The microcolumns in the *x*, *y*-plane of a grain boundary. The full lines represent the layers belonging to the smectic blocks above and beneath the grain boundary. The dashed lines represent the dispiration lines. The arrows and dotted or crossed circles indicate the *c*-director in the grain boundary.

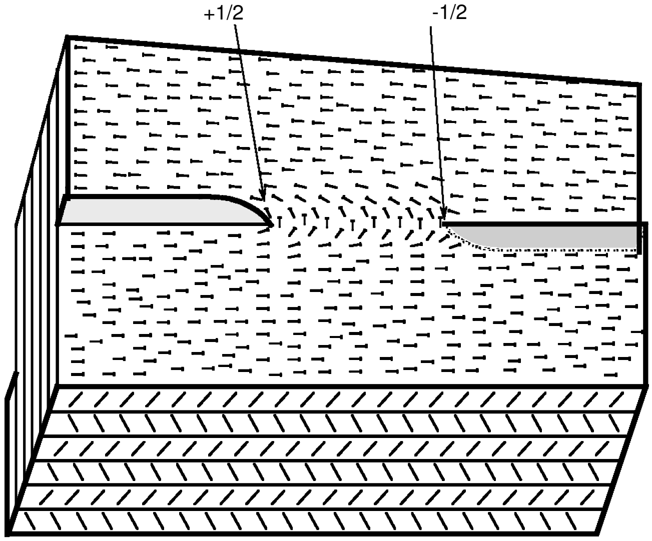

Figure 11. The *c*-director field in the vicinity of a grain boundary viewed in the *x*, *z*-plane.

From the drawing in figure 11 it is obvious that in the grain boundary between each pair of one + 1/2 and one − 1/2 dispiration, the *c*-director, and hence the tilt plane, is locally parallel to the TGB helix. When an electric field is applied along the helix, there are already regions where the tilt plane is locally along the field and, hence, where $\mathbf{P}_s \times \mathbf{E} \neq 0$. As the lowest energy density is achieved when the tilt plane is along the field, these regions in the vicinity of the grain boundaries tend to grow, without threshold, pushing the dispirations away from each other. At the same time the regions of the grain boundary in which the tilt plane is parallel to the boundary will shrink. This means that we should introduce two lengths, l_{d1} and l_{d2}, corresponding to the distances between two dispirations between which the tilt plane is, respectively, perpendicular and parallel to the grain boundary. The applied field will increase l_{d1} and decrease l_{d2}, and when l_{d2} becomes small enough the screw dislocations on either side of l_{d2} vanish. This makes the total number of screw dislocations decrease and, assuming a more or less constant thickness of the smectic slabs, thereby makes the pitch of the $TGBC_A$ phase increase. This is in agreement with our experimental observation where the pitch increases prior to the transformation into the focal-conic texture on applying an electric field. This picture of course holds only if the smectic layer normal is perpendicular to the $TGBC_A$ helix axis which was confirmed by results from preliminary X-ray experiments [23].

The formation of either the Grandjean or the focal-conic texture in TGBA and TGBC phases has been discussed by Galerne [22] as mainly dependent on the balance of the elastic constants associated with the block thickness and the dislocation line distance in the grain boundaries. Two extreme cases were distinguished: (i) l_b is a much more adjustable length than l_d, and the opposite (ii) l_d is more adjustable than l_b. The first case results in a TGB phase built-up of developable domains. The second case results in an arrangement of basically parallel layers of smectic slabs, which should therefore exhibit a focal-conic texture. In our case, l_d (or rather l_{d1} and l_{d2}) seems to vary in the presence of an electric field and when the pitch becomes long enough focal-conic domains could in principle develop. However, according to our model, before this happens there is in the $TGBC_A$ phase of the compound studied a field-induced reorientation of the TGB helix from being perpendicular to parallel to the cell surfaces.

5. Conclusions

Based on the field-induced texture transformations and their electro-optic response we have been able to deduce a model of the microscopic organization of the $TGBC_A$ phase both within the smectic slabs and in the vicinity of the grain boundaries. The model presented explains the electric field-induced increase of the pitch of the helicoidal axis as well as the field-induced transformation from the Grandjean into the focal-conic texture. The anticlinic structure of the smectic slabs of the $TGBC_A$ phase requires that the grain boundaries consist of a regular lattice of dispirations. Such a discontinuity requires a unit screw dislocation combined with a half-unit dislocation. This is different from TGBA and TGBC phases where pure screw dislocations form the grain boundary. Inside the slabs of the $TGBC_A$ phase, the tilt plane is perpendicular to the helix axis. The observed effects are due to the field-induced reorientation of the tilt plane of the local anticlinic structure.

One might ask if an array of screw dislocations with a Burger's vector of *two* unit layers could be an alternative model for mediating the twisting blocks shown in figure 11. However, the fact that the elastic energy is already quadratic in the Burger's vector, does not make this seem probable. Furthermore, we know already that the dispiration with unit Burger's vector is an inherent feature of the SmC_A^* phase. Finally only the dispiration gives a simple explanation for the observed $TGBC_A$ behaviour in an electric field.

We thank G. Andersson for many fruitful discussions and would like to acknowledge financial support from the EU TMR program ORCHIS, the Swedish Foundation for Strategic Research and the University of Hull Overseas Research Student Scheme.

References

[1] De Gennes, P. G., 1972, *Solid State Commun.*, **10,** 753.
[2] Renn, S. R., and Lubensky, T. C., 1988, *Phys. Rev. A*, **38,** 2132.
[3] Goodby, J. W., Waugh, W. A., Stein, S. M., Chin, E., Pindak, R., and Patel, J. S., 1989, *Nature*, **337,** 449.
[4] Goodby, J. W., Waugh, W. A., Stein, S. M., Chin, E., Pindak, R., and Patel, J. S., 1989, *J. Am. Chem. Soc.*, **111,** 8119.
[5] Srajer, G., Pindak, R., Waugh, M. A., Goodby, J. W., and Patel, J. S., 1990, *Phys. Rev. Lett.*, **64,** 1545.
[6] Renn, S. R., 1992, *Phys. Rev. A*, **45,** 953.
[7] Nguyen, H. T., Bouchta, A., Navailles, L., Barois, P., Isaert, N., Twieg, R. J., Maaroufi, A., and Destrade, C. J. 1992, *J. Phys. II (Fr.)*, **2,** 1889.
[8] Navailles, L., Barois, P., and Nguyen, H. T., 1993, *Phys. Rev. Lett.*, **71,** 545.
[9] Takatoh, K., Lamb, A. G. M., and Goodby, J. W., unpublished results.
[10] Pramod, P. A., Pratibha, R., and Madhusudana, N. V., 1997, *Curr. Sci.*, **73,** 761.
[11] Goodby, J. W., Nishiyama, I., Slaney, A. J., Booth, C. J., and Toyne, K. J., 1993, *Liq. Cryst.*, **14,** 37.
[12] Goodby, J. W., Petrenko, A., Hird, M., Lewis, R. A., Meier, J., and Jones, J. C., 2000, *Chem. Commun.*, 1149.
[13] Petrenko, A. S., Hird, M., Lewis, R. A., Meier, J. G., Jones, J. C., and Goodby, J. W., 2000, *J. Phys.: Condens. Matter*, **12,** 8577.
[14] Ribeiro, A. C., Nguyen, H. T., Galerne, Y., and Guillon, D., 2000, *Liq. Cryst.*, **27,** 27.
[15] Bennemann, D., Heppke, G., Levelut, A. M., and Lötzsch, D., 1995, *Mol. Cryst. Liq. Cryst.*, **260,** 351.

[16] Levelut, A. M., Hallouin, E., Bennemann, D., Heppke, G., and Loetzsch, D., 1997, *J. Phys. II*, **7,** 981.

[17] Fukuda, A., Takanishi, Y., Isozaki, T., Ishikawa, K., and Takezoe, H., 1994, *J Mater. Chem.*, **4,** 997.

[18] Shiyong, Z., Bing, W., Keast, S. S., Neubert, M. E., Taylor, P. L., and Rosenblatt, C., 2000, *Phy. Rev. Lett.*, **84,** 4140.

[19] Qian, T., and Taylor, P. L., 1999, *Phys. Rev. E*, **60,** 2978.

[20] Rudquist, P., Lagerwall, J. P. F., D'havè, K., Meier, J. G., and Lagerwall, S. T. (to be published).

[21] Lagerwall, S. T., 1999, *Ferroelectric and Antiferroelectric Liquid Crystals* (Weinheim: Wiley-VCH).

[22] Galerne, Y., 1994, *J. Phys. II*, **4,** 1699.

[23] Meier, J. G., Nobili, M., Brunet, M., Petrenko, A. S., Goodby, J. W., and Lagerwall, S. T. (to be published).